UNIVERSITY OF THESSALY

SCHOOL OF ENGINEERING

DEPARTMENT OF ELECTRICAL AND COMPUTER ENGINEERING

Classification of Wireless Communication Signals

Diploma Thesis

Apostolos Pappas

Supervisor: Antonios Argyriou

Volos 2020

UNIVERSITY OF THESSALY

SCHOOL OF ENGINEERING

DEPARTMENT OF ELECTRICAL AND COMPUTER ENGINEERING

Classification of Wireless Communication Signals

Diploma Thesis

Apostolos Pappas

Supervisor: Antonios Argyriou

Volos 2020

ΠΑΝΕΠΙΣΤΗΜΙΟ ΘΕΣΣΑΛΙΑΣ

ΠΟΛΥΤΕΧΝΙΚΗ ΣΧΟΛΗ

ΤΜΗΜΑ ΗΛΕΚΤΡΟΛΟΓΩΝ ΜΗΧΑΝΙΚΩΝ ΚΑΙ ΜΗΧΑΝΙΚΩΝ ΥΠΟΛΟΓΙΣΤΩΝ

Κατηγοριοποίηση Σημάτων Ασύρματης Επικοινωνίας

Διπλωματική Εργασία

Απόστολος Παππάς

Επιβλέπων/πουσα: Αντώνιος Αργυρίου

Βόλος 2020

Approved by the Examination Committee:

Supervisor **Antonios Argyriou**
Associate Professor, Department of Electrical and Computer Engineering, University of Thessaly

Member **Gerasimos Potamianos**
Associate Professor, Department of Electrical and Computer Engineering, University of Thessaly

Member **Athanasios Korakis**
Associate Professor, Department of Electrical and Computer Engineering, University of Thessaly

Date of approval: 20-9-2020

Acknowledgements

First and foremost, I would like to express my deepest appreciation to my thesis supervisor Dr. Antonios Argyriou, for inspiring me towards the completion of this thesis. His trust, guidance and support, even when seeing me struggling at times, are only a few of the traits that I will be forever thankful for. Letting me express my ideas, and often seeing them fail, gave me some of the most important lessons I ever got.

I would also like to thank Emeritus Professor Dr. Elias Houstis. Apart from the valuable knowledge gained from his teaching, his trust in me gave me confidence in a field where I most needed it. His continuous passion for learning and teaching never fails to inspire me to the fullest.

Of course none of these would be ever possible without the never ending support and love gained from my family, and especially from my parents, Konstantinos and Kornilia. I was fortunate to be raised watching them set the best of examples in every aspect of life. To this day, I am extremely grateful to be your son.

Last but not least, I am deeply indebted to those who stood by me in the darkest of times. To those who liked me at my best and loved me at my worst. To those who helped me get on my feet, even though being down. To my friends.

> I don't like honors. I've already got the prize. The prize is the pleasure of finding the thing out, the kick in the discovery, the observation that other people use it. Those are the real things. The honors are unreal to me.
>
> *Richard P. Feynman*

DISCLAIMER ON ACADEMIC ETHICS AND INTELLECTUAL PROPERTY RIGHTS

«Being fully aware of the implications of copyright laws, I expressly state that this diploma thesis, as well as the electronic files and source codes developed or modified in the course of this thesis, are solely the product of my personal work and do not infringe any rights of intellectual property, personality and personal data of third parties, do not contain work / contributions of third parties for which the permission of the authors / beneficiaries is required and are not a product of partial or complete plagiarism, while the sources used are limited to the bibliographic references only and meet the rules of scientific citing. The points where I have used ideas, text, files and / or sources of other authors are clearly mentioned in the text with the appropriate citation and the relevant complete reference is included in the bibliographic references section. I fully, individually and personally undertake all legal and administrative consequences that may arise in the event that it is proven, in the course of time, that this thesis or part of it does not belong to me because it is a product of plagiarism».

The declarant

Apostolos Pappas
15-9-2020

Abstract

With the ongoing development in the telecommunications field, new technologies emerge, raising the bar in security demands.The Internet of Things (IoT), advancement in satellite, civil and military communications provide applications sensitive to adversarial attacks. In this paper, we explore the concept of signal classification as a means towards transmitter configuration identification. The topics of modulation and number of transmitter antennas classification are initially examined independently and then combined in a joint classifier, able to achieve accuracy up to 90% in certain Signal to Noise Ratio (SNR) conditions. To achieve these results, two different types of classifiers, equipped with a variety of Machine Learning (ML) algorithms, are proposed based on the way the antennas are classified.

Περίληψη

Με τη ολοένα συνεχόμενη ανάπτυξη στον τομέα των τηλεπικοινωνιών, νέες τεχνολογίες αναδύονται και αυξάνουν τις απαιτήσεις στον τομέα της ασφάλειας. Το Διαδίκτυο των Πραγμάτων (Internet of Things), η πρόοδος στις δορυφορικές, πολιτικές και στρατιωτικές επικοινωνίες παρέχουν εφαρμογές ευαίσθητες σε εχθρικές επιθέσεις ασφαλείας. Σε αυτό το άρθρο, διερευνούμε την έννοια της ταξινόμησης σήματος ως μέσο για την αναγνώριση διαμόρφωσης πομπού. Τα θέματα της διαμόρφωσης και της κατηγοριοποίησης του αριθμού των κεραιών πομπού, εξετάζονται αρχικά ανεξάρτητα και στη συνέχεια συνδυάζονται σε έναν κοινό ταξινομητή, ικανό να επιτύχει ακρίβεια έως και 90 % σε ορισμένες συνθήκες λόγου σήματος προς θόρυβο (Signal to Noise Ratio). Για να επιτευχθούν αυτά τα αποτελέσματα, προτείνονται δύο διαφορετικοί τύποι ταξινομητών, εξοπλισμένοι με μια ποικιλία αλγορίθμων Machine Learning (ML) βασιζόμενοι στον τρόπο κατηγοριοποίησης του αριθμού των κεραιών πομπού.

Table of contents

List of figures

List of tables

Abbreviations

AIC	Akaike Information Criterion
ALRT	Average-Likelihood-Ratio-Test
AMC	Automatic Modulation Classification
AWGN	Additive White Gaussian Noise
CSI	Channel Side Information
EW	Electronic Warfare
ET	Extra Trees
FB	Feature-Based
GLRT	Generalized-Likelihood-Ratio-Test
HLRT	Hybrid-Likelihood-Ratio-Test
HOCs	High Order Cumulants
HOMs	High Order Moments
IoT	Internet of Things
ISI	Inter Symbol Interference
kNN	k-Nearest-Neighbors
LA	Link Adaptation
LB	Likelihood-Based
LTI	Linear Time Invariant
LoS	Line of Sight
LRT	Likelihood-Ratio-Test
MDL	Minimum Description Length
MIMO	Multiple-Input and Multiple-Output
MRC	Maximal-Ratio Combining
MSE	Mean Squared Error
OFDM	Orthogonal Frequency-Division Multiplexing

PSK	Phase Shift Keying
QAM	Quadrature amplitude modulation
RF	Radio Frequency
RF	Random Forest
Rx	Receiver
SISO	Single Input and Single Output
Tx	Transmitter
VHOS	Very High Order Statistics

Chapter 1

Introduction

Classification of wireless communication signals is a multidimensional concept with emphasis on the classification of the way that the transmitted signal is modulated. While most of the related work focuses on the latter part, it is important to think of signal classification as a potentially multi-step process.

In this thesis, we examine the potential of deep learning in a blind scenario. In that way, both the modulation classification and the classification of the number of Tx antennas problems are examined.

1.1 Automatic Modulation Classification

In a modern communications system, the type of modulation used has a great impact on various aspects of its performance and security. As mentioned in [2], different modulations provide different levels of noise immunity, data rate, and robustness in various transmission channels. In order to demodulate the modulated signals and to recover the transmitted message, the receiving end of the system must be equipped with the knowledge of the modulation type. However, that knowledge is not to be taken for granted. In that case, the receiver is to be considered as blind and new methods of demodulation should be taken into account.

Automatic Modulation Classification (AMC) is increasingly important as the number and sophistication of digital signaling systems increase [3]. That results in a great need of having reliable intelligent models to distinguish between various signals. AMC's ultimate goal is to detect and classify the way an unknown received signal is modulated. In that way, a so called *blind* receiver can guarantee the correct demodulation and, in some cases, the recovery

of the transmitted signal. In the real world, applications that require a form of modulation classification can be found in both civil and military environments.

In a civil scenario, AMC can be used in applications such as Link Adaptation. Considering a LA scene, where having matching modulations is of high importance, the transmitter can be replaced by a adaptive modulation unit. Even though LA seems to be the most important of AMC's civil applications, in [4] the authors examine the modulation classification problem for a distributed wireless spectrum sensing network. In their work AMC is an integral part of spectrum enforcement since such a classifier can assist in identifying suspicious transmissions.

Research in the military scene establishes AMC as an important asset in the field of Electronic Warfare (EW). The applications vary from recovering the transmitted signal between adversary units to even locating them. For example, in [5], it is mentioned that EW equipment should be capable of not only detecting and identifying the received signal, but locating it as well. In that way, jamming responses and countermeasures can be generated efficiently. An example of a detection and Electronic Attack (EA) application in a military scenario can be found in Figure 1.1.

The AMC scheme is well documented throughout the available literature, since plenty of research over the years is focused on recognizing the modulation type of an incoming signal. In [6], the reader can have an extensive report on numerous AMC approaches and applications. Most of the work is focused on the different approaches on modulation classification. The differentiation between various methods proposed, can be found mainly in the algorithms proposed, as well as in their input type. With the continuous development of Deep Learning algorithms (DL), many of their applications can be found in the physical layer [7]. A number of DL methods, both supervised and unsupervised, where developed towards AMC [8, 9, 10, 11, 12, 13]. In [3] and [1], hierarchical classifiers are proposed using statistical features extracted from the incoming signal.

1.2 Number of Antennas Classification

A second idea related to signal classification, that is studied to a lesser extend, is the identification of the number of antennas used by the transmitter. This knowledge can have a crucial impact on the modulation classification performance. For example, consider scenarios where

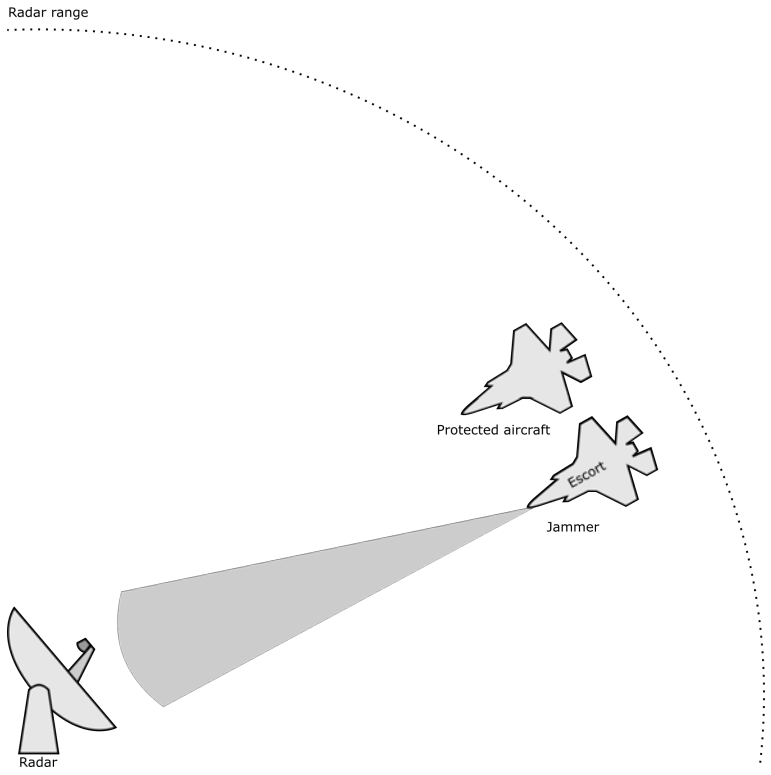

Figure 1.1: Jamming EA application

the transmitter uses multiple antennas. If a single antenna is present in the receiver, symbol interference is inevitable. Thus, the classification performance might be affected negatively.

In scenarios where the communication between the transmitter and the receiver is established, this type of classification could be vital regarding the energy consumption levels. When Maximal-Ratio Combining (MRC) is not necessary, using a small (or even a single) number of antennas can be proven very energy-efficient. In Multiple-Input and Multiple-Output (MIMO) systems, dynamic antenna selection is another method that can be helpful in managing energy efficiency [14]. Additionally, receiving antenna redundancy can be proven useful in some applications. Moreover, the design of the preamble structure for MIMO channel estimation in an ad-hoc system depends on the number of transmit antennas in the system [15]. In military communications, this scheme introduces more challenges regarding cognitive radios and surveillance systems.

1.3 Related Work

Signal Classification is not a new challenge in the Communications and ML fields. In space missions that are being developed with automation as an essential part of them, the

creation of autonomous radios that can receive signals without a priori knowledge of their characteristics is of high importance. This is evident in [16].

Regarding the number of antennas detection procedure, approaches exploiting pilot patterns have been followed in [17, 18, 15] examining cooperative scenarios with cognitive receivers. In a non-cooperative scheme, this type of classification is present in [19] and done with the use of the Akaike Information Criterion (AIC) and the Minimum Description Length (MDL) estimators. Although both AMC and antenna detection are studied separately, to our knowledge, only one work examines these two problems in a joint manner. In their work [20], Merve Turan et al. proposed a decision theoretic approach for spatial multiplexing MIMO systems considering the modulation classification and the antenna detection as a joint problem in a non-cooperative scenario. The aforementioned joint problem is dealt with by minimizing the extended MDL criterion.

Chapter 2

System Model

2.1 Modeling the Communications System

Over the past decades, Wireless Communication has evolved in a great extend so as to meet an on-going demand for high and efficient data rates. Many systems have emerged having both indoor and outdoor applications. That transition, from wired to wireless communication, added a whole lot of new parameters in the modeling equation. From weather conditions, to the relative motion between the transmitter and the receiver, there is a plethora of characteristics that affect our signal. It is, thus, understandable that the knowledge of the aforementioned characteristics plays a major role in not only theoretically modeling the system but also in designing it. In general, when trying to model a wireless Communications System, one can divide it into three main parts:

- the Transmitter
- the Channel and
- the Receiver

That high level configuration, which we are using throughout this paper, can be seen in Figure 2.1. Based on the figure, a Communications System can be mathematically modeled as follows

$$\mathbf{y}(t) = H(t)\mathbf{x}(t) + \mathbf{n}(t)$$

In the above equation, $y(t)$ can be perceived as the received signal at the *t*-th sampling time. It is the result of the channel's time variant modification, $\mathbf{H}(t)$, of the transmitted signal, $x(t)$, plus the Additive White Gaussian Noise (AWGN), which is denoted as $n(t)$ in our equation.

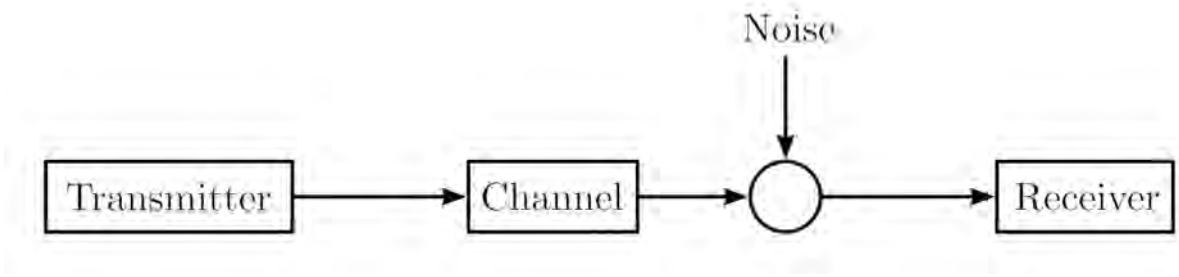

Figure 2.1: Simplified block diagram of a Communications System

Raw bits are encoded by the transmitter. In our case Grey encoding is used. Next, the bits are converted to complex baseband symbols. Both the real and imaginary parts of the baseband signal are filtered through the transmitter (Tx) filter. For this work the filter is chosen to be a square pulse, where its impulse response is determined by the oversampling factor and its amplitude is adjusted so that the energy per bit is constant regardless of the oversampling selected. The next step is the conversion of the previous information into an analog waveform suitable for transmission. That process, where one of the properties of the periodic analog signal (the carrier wave) like amplitude, phase or the frequency is altered according to the message signal (baseband signal) is called *modulation*.

A transmitted signal, being an electromagnetic Radio Frequency (RF) one, is highly affected by the medium that it is transmitted through. As a result, it might be reflected, diffracted or scattered. Other characteristics of the medium that highly affect the signal can be traced in the atmospheric conditions, the relative mobility between the transmitters and the receivers, types of antennas used etc. In [21], David Tse and Pramod Viswanath refer to the fading phenomenon as one of the two most fundamental aspects of wireless communication. The second aspect is the interference between wireless users as a result of the non existent isolation in the wireless point-to-point communication. Thus, the reader can realise the importance of modeling the channel. In the applications examined though out this paper, the existence of a fading channel, on its own, adds another level of complexity to the classification problem.

We consider flat fading channels which means that the channel can be modeled with a single tap, while the PDF of the random channel is assume to follow a Rayleigh distribution [21]. This channel is modeled as a complex number composed by two zero mean Gaussian random values. In the case where both the transmitter and the receiver have one antenna (as can be seen in Figure 2.2), the channel is represented by a scalar random complex value $h = a + bj$. Assuming that a and b are independent normal random values, it stands that

$h \sim CN(0, \frac{1}{\sqrt{2}})$. A channel like the one mentioned is also referred to as Single Input and Single Output (SISO) channel.

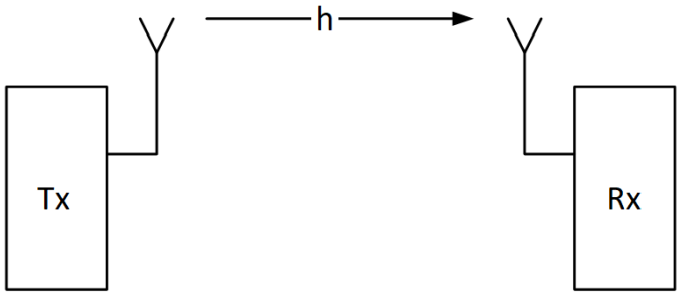

Figure 2.2: Topology of a SISO channel.

Thus, when transmitting K symbols, the vectorized representation of the channel is the following:

$$\begin{bmatrix} Y_1 \\ Y_2 \\ \vdots \\ Y_K \end{bmatrix} = h(t) \begin{bmatrix} s_1 \\ s_2 \\ \vdots \\ s_K \end{bmatrix} + \begin{bmatrix} n_1 \\ n_2 \\ \vdots \\ n_K \end{bmatrix}$$

When the transmitting and the receiving part of the system are equipped with multiple antennas, the system is characterized as a MIMO one. Each set of antennas is modeled with a new complex number h_{ij} and overal MIMO model can be seen in Figure 2.3. In this case $\mathbf{H(t)}$ is an $N \times M$ matrix. We, thus, have:

$$H(t) = \begin{bmatrix} h_{11}(t) & h_{12}(t) & \dots & h_{1M}(t) \\ h_{21}(t) & h_{22}(t) & \dots & h_{2M}(t) \\ \vdots & \vdots & \ddots & \vdots \\ h_{N1}(t) & h_{N2}(t) & \dots & h_{NM}(t) \end{bmatrix}$$

The corresponding vector form of the channel is:

$$\begin{bmatrix} Y_i \\ Y_{i+1} \\ \vdots \\ Y_{i+N-1} \end{bmatrix} = \begin{bmatrix} h_{11}(t) & h_{12}(t) & \dots & h_{1M}(t) \\ h_{21}(t) & h_{22}(t) & \dots & h_{2M}(t) \\ \vdots & \vdots & \ddots & \vdots \\ h_{N1}(t) & h_{N2}(t) & \dots & h_{NM}(t) \end{bmatrix} \begin{bmatrix} x_k \\ x_{k+1} \\ \vdots \\ x_{k+M-1} \end{bmatrix} + \begin{bmatrix} n_i \\ n_{i+1} \\ \vdots \\ n_{i+N-1} \end{bmatrix}$$

One can easily realize that the defined $\mathbf{H}(t)$ matrix will be square when the communicating parts of the system use the same number of antennas. Additionally, in that case, the received signal vector has the same dimensions as the originally transmitted one. On the other hand, when an inequality between the number of antennas is spotted ($M \neq N$), the corresponding "channel" matrix will be orthogonal. In the course of this paper, there are cases that concern a type of system where the number of transmitting antennas is N, while the receiving part is equipped with only one. This system is known as a Multiple-Input and Single Output (MISO) system. Hence, the channel is modeled as a $1 \times N$ vector, that is multiplied with the corresponding N symbols. Note that this type of channel is prone to symbol interference at the receiver. Modeling this special case in vector form is a subtractive version of the MIMO one.

$$Y_i = \begin{bmatrix} h_{11}(t) & h_{12}(t) & \dots & h_{1M}(t) \end{bmatrix} \begin{bmatrix} x_k \\ x_{k+1} \\ \vdots \\ x_{k+M-1} \end{bmatrix} + n_i$$

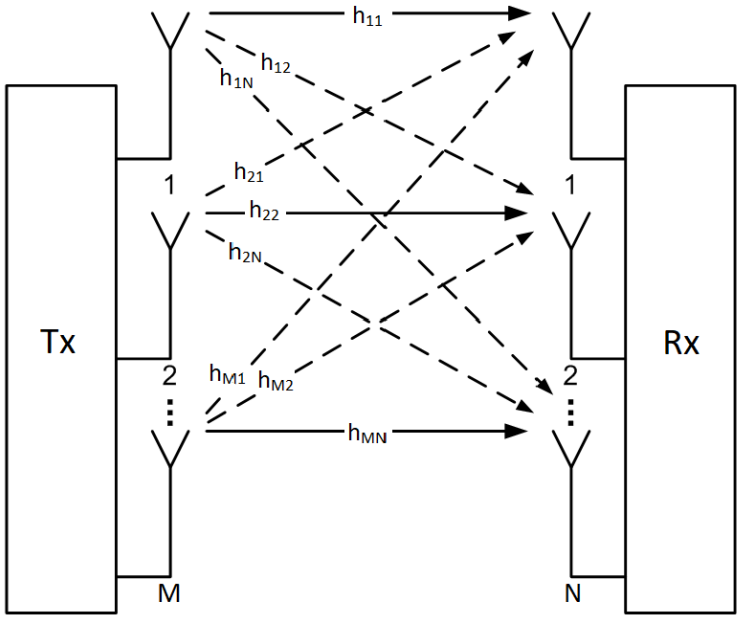

Figure 2.3: Topology of a $M \times N$ MIMO channel.

It is, of course, worth noting that the effect of the channel (i.e multiplying with a complex number) can be found both in the amplitude and the phase of the transmitted signal. The reader can observe this effect in Figure 2.4 where phase shift illustrated for a QPSK modulation.

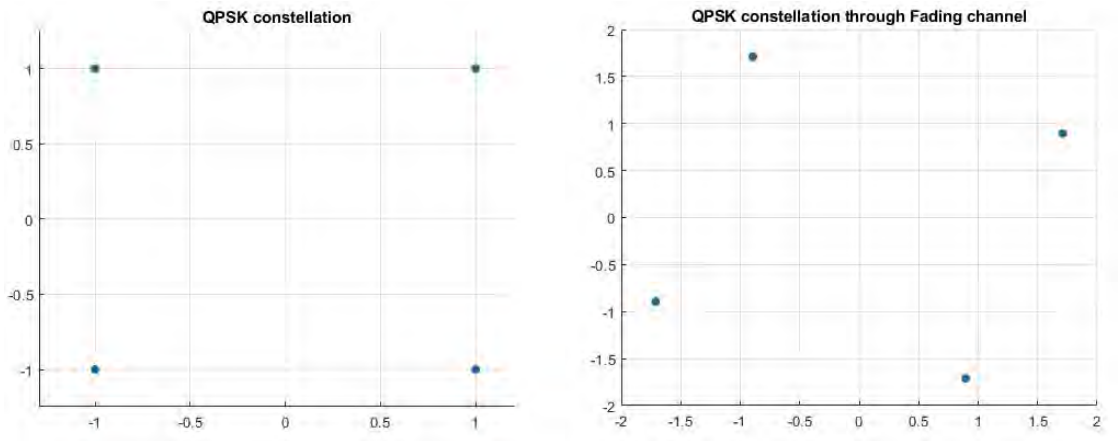

Figure 2.4: The effect of fading in the QPSK constellation

In this paper, the thermal noise that affects the transmitted signal is considered to be Additive White Gaussian Noise (AWGN). As such, $n(\cdot)$ is a zero mean Gaussian random value ,$n(\cdot) \sim \mathcal{CN}(0, N_0)$, which is uncorrelated with $\{x_k\}$. Another property induced by the fact that the thermal noise is white, is that $E[n(t_1)n(t_2)] = \sigma^2\delta(\tau)$, where $\tau = t_2 - t_1$.

2.2 MATLAB Based Simulator

Throughout this work, the feature extraction process is solely based on the raw I/Q data composing the received signal $\mathbf{y(t)}$. Therefore, the creation of a corresponding simulator covering the needs of the described system was of high importance. Reflecting the significance of the channel in a communications system as detailed in 2.1, a large proportion of effort was put into simulating it. Using MATLAB programming language, a combined transmitter and channel simulator was constructed. During its design, scalability and reusability were largely considered, as a result of the multiple and different experiments run in the span of this thesis. A more generalized form of the proposed simulator can be seen in Figure 2.5.

2.2.1 The transmitter

Starting off with the transmitter part of the simulator, the first step of any iteration is to generate the random bits to be transmitted over the channel. Depending on the type of the modulation chosen by the user, zero padding is performed in the bit vector if necessary. Following the zero padding, gray coding is applied just before modulating the bits into the desired symbols. In this way, the symbol vector $\mathbf{x(t)}$ mentioned in 2.1 is created. It is this

vector that will later be distorted by the communications channel. An option for Orthogonal Frequency-Division Multiplexing (OFDM) is also offered but not used in this thesis. In the Tx filter, convolution is performed by a square pulse having a magnitude of $\sqrt{\frac{E_b}{os}}$ and length of os, where os is the desired oversampling value. The effect of oversampling at the transmitter filter can be observed in Figure 2.6. In Table 2.1, the reader can have a detailed overview of the parameters regarding the transmitter part of the simulator.

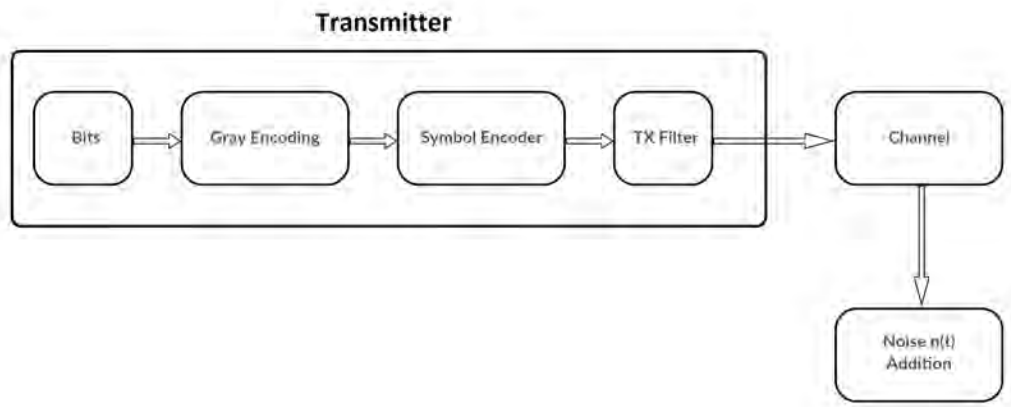

Figure 2.5: Topology of the Transmitter including the channel.

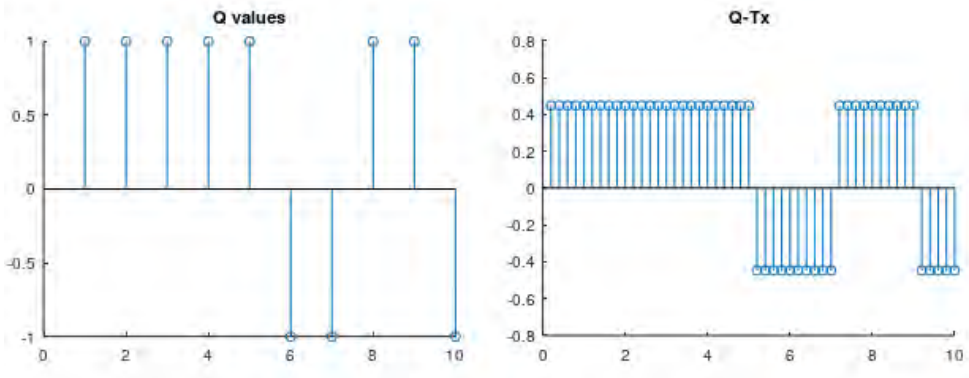

Figure 2.6: The output of the Tx filter with $E_b = 1$ and $os = 5$.

id	Parameter	Description
1	Rb	Bit rate (b/s)
2	Eb	Energy per bit
3	os_value	Oversampling factor
4	nbits	Number of bits to be transmitted
5	ofdm	(Boolean) Use of OFDM
6	n_subcarriers	No. total subcarriers (without cyclic prefix)
7	cyclic_prefix	No. subcarriers composing the cyclic prefix

Table 2.1: List of Tx input parameters along a short description.

2.2.2 The communication channel

It is obvious in subsection 2.1, that modeling the distortion induced by the communications system in a fading channel is a crucial part of this thesis. Because of the signal propagation in space, reflections are unavoidable. Consequently, the receiver receives multiple and delayed distorted copies of the transmitted signal through time. This phenomenon is the cause of another unwanted event called Inter Symbol Interference (ISI) that negatively effects the received signal, making the communication less reliable. It is common to simulate channels as Linear Time Invariant (LTI) systems having certain magnitude and duration. In this way, each instance of the channel $\mathbf{h(t)}$ in a SISO channel, will be a vector containing the impulse response of the corresponding channel. Thus, the effect of the channel can be modeled by performing the convolution operation between the transmitted symbols and the channel impulse response vector. In the case where multiple antennas are present, such as in MIMO systems, the corresponding convolution procedure can be simulated by equipping Toeplitz matrices. A corresponding channel response can be examined in Figure 2.7. In this work, we simplify things by making the assumption of having only Line of Sight (LoS) communication. In this scenario, transmit and receive stations are in view of each other without any sort of an obstacle between them. This fact cancels the delay spread caused by reflection in obstacles, annihilating the effect of ISI. Hence, the process of simulating the fading channel effect is reduced into multiplying $\mathbf{x(t)}$ with the corresponding channel's complex value.

Following the methodology mentioned in the previous section, the transmitted signal vec-

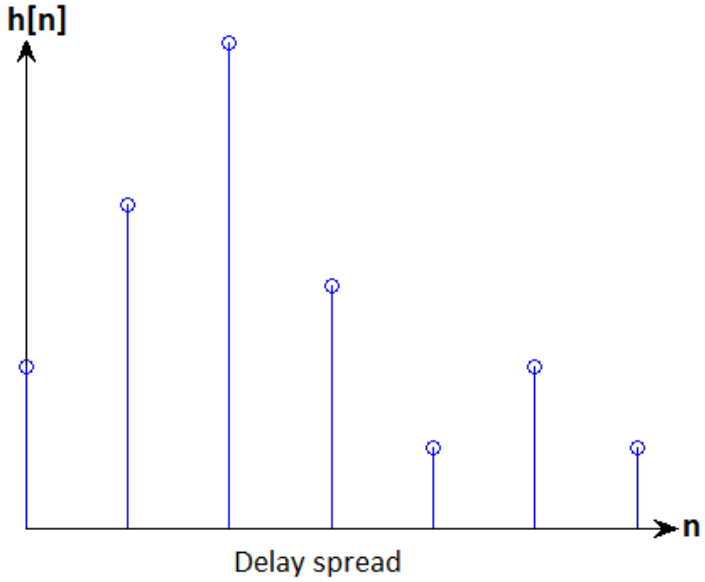

Figure 2.7: Representative impulse response of a frequency selective channel.

tor is shifted and multiplied with the corresponding matrix (MIMO), vector (MISO) or scalar (SISO) value. This procedure affects highly the dimension of the $\mathbf{y}$ vector and might introduce interference from other symbols. Another issue to consider is the alteration of the communications channel through time. To simulate this occurrence, both the channel period and the symbol rate are taken into consideration. Simply dividing the channel period by the corresponding symbol one can provide insight into the number of symbols that will be transmitted during a certain channel state before it changes. As a last step, the thermal AWGN noise addition is done directly by creating the respective noise vector that matches the dimensions of $\mathbf{y}$. A detailed presentation of this simulator's tunable parameters regarding the modeling of the channel can be found in Table 2.2.

id	Parameter	Description
1	T_channel	Channel period
2	transmitter_antennas	No. transmitter's antennas
3	receiver_antennas	No. receiver's antennas
4	channel_type	Channel type
5	equalization	(Boolean) Equalization application

Table 2.2: List of Rx input parameters along a short description.

2.3 Receiver & Feature Extraction

2.3.1 Receiver Functionality

In this section, we introduce the receiver functionality. The receiver examined in this thesis does perform any kind of channel equalization or demodulation. This is because our receiver has no knowledge regarding the used modulation at the Tx. It is important to think of the receiver as blind having no a-priori Channel Side Information (CSI). Independently of the application, either trying to identify the transmitter topology or adapt itself to new transmission protocols, the first task performed by the receiver is feature extraction. Feature extraction is necessary for the ML or DL algorithms used for the classification process. After classifying the incoming signal, the receiver will be able to perform other tasks such as demodulating the signal, re-configuring itself to match the needs of its communication with the transmitter and even estimating the channel using pilots induced by a cooperative transmitter.

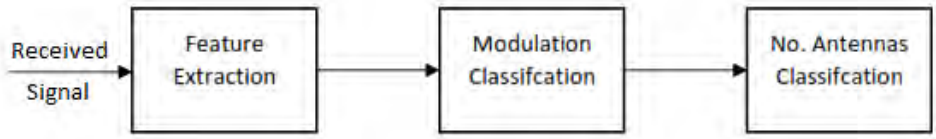

Figure 2.8: Receiver functionality flow graph.

The signal classification performed by the receiver module is composed of two phases. In the first phase, the receiver is responsible of classifying the modulation of the incoming signal. This first step highly impacts the signal classification performance. Having recognized the way that the received signal is modulated, the next step is to classify the number of transmitting antennas. The proposed hierarchical classification procedure is described in Figure 2.8. In the next two chapters of this thesis, the two stages of the signal classification performed by the receiver are examined at first as independent tasks. In Chapter 5, the two phases are combined into the proposed detector.

2.3.2 Feature extraction

It is well documented that, in general, AMC algorithms can be categorized into two groups, the Likelihood-Based (LB) and the Feature-Based (FB) schemes. The way in which

the LB schemes cope with the AMC problem is by equipping methods such as the Generalized-Likelihood-Ratio-Test (GLRT), the Average-Likelihood-Ratio-Test (ALRT), the Hybrid-Likelihood-Ratio-Test (HLRT) as well as other variations of the LRT. Regarding the FB approach, a big advantage in following it is the simplicity of its implementation as well as the performance which approaches the one achieved by the LB schemes. In [22, 6] one can have a detailed report on various methods based on the LB approach. A plethora of different features is proposed regarding FB algorithms, ranging from raw signal characteristics [23, 24, 25, 26, 27] to other statistically extracted features. The latter type comprises of features such as high order moments (HOMs) [28, 3], high order cumulants (HOCs) [29], very high order statistics (VHOS) [30] and others [31].

To perform the signal classification in this work, HOCs were used as features fed into the ML and DL models. HOCs can be thought of as functions containing HOMs. In this work, HOMs extracted from the unknown received signal are calculated as shown bellow:

$$M_{pq} = E[\mathbf{y}^{p-q}(\mathbf{y}^*)^q]$$

The above equation describes the pth order moment as computed using the complex-valued received signal y. Continuing, the HOCs expression based on HOMs is described.

$$Second\ Order\ Cumulants \begin{cases} C_{20} = M_{20} \\ C_{21} = M_{21} \end{cases}$$

$$Fourth\ Order\ Cumulants \begin{cases} C_{40} = M_{40} - 3M_{20}^2 \\ C_{41} = M_{40} - 3M_{20}M_{21} \\ C_{42} = M_{42} + |M_{40}|^2 - 2M_{21}^2 \end{cases}$$

$$SixthOrderCumulants \begin{cases} C_{60} = M_{60} - 15M_{20}M_{40} + 30M_{20}^3 \\ C_{61} = M_{61} - 5M_{21}M_{40} - 10M_{20}M_{41} + 30M_{20}^2M_{21} \\ C_{62} = M_{62} - 6M_{20}M_{42} - 8M_{21}M_{41} - M_{22}M_{40} + 6M_{20}^2M_{22} + 24M_{21}^2M_{20} \\ C_{63} = M_{63} - 9M_{21}M_{42} + 12M_{21}^3 - 3M_{20}M_{43} - 3M_{22}M_{41} \\ +18M_{20}M_{21}M_{22} \end{cases}$$

As proposed in [32], HOCs are normalized having each cumulant raised to the power of $\frac{2}{p}$. Additionally as done in [1], the magnitudes of the corresponding cumulants are used as actual input to the ML and DL models.

2.3.3 Dataset creation

The first step of the experiments conducted through chapters 3 to 5, is the simulation procedure which provides the necessary dataset as described in 2.3.2. Experiments were performed using two different datasets. Each dataset was produced using 1, 2 and 4 Tx antennas, transmitting 1024 symbols modulated in six different ways. The samples per symbol is set to one and 600 samples of each modulation and Tx antennas number combination were taken. The number of Rx antennas equipped is what differentiates the two datasets. In the first dataset the receiver is equipped with one antenna, while in the second one two Rx antennas are present. In addition, the number of channel realizations is the same for each bunch of transmitted symbols and equal to 21. For simplicity, we refer to the dataset with one Tx antenna as *Dataset 1* and use the term *Dataset 2* for the one where two antennas are present in the transmitter. Hence, each one of them has the following form (Table 2.3):

C_{20}	C_{21}	C_{40}	C_{41}	C_{42}	C_{60}	C_{61}	C_{62}	C_{63}	Modulation	Tx antennas
Numerical (Used as input features)									Nominal (Used as Classes)	

Table 2.3: Dataset description.

Chapter 3

Modulation classification

For this chapter, we first reproduced the work of Abdelmutalab et al [1]. Throughout their work, a hierarchical structure is presented classifying between six types of modulation. These six types are: BPSK, QPSK, 8-PSK, 16-QAM, 64-QAM and 256-QAM. Additionally, a form of preprocessing is applied to the cumulant features other than their normalization. These obtained features are expanded into a higher dimensional space by a second degree polynomial fit.

3.1 The Hierarchical Scheme

Due to the hierarchical structure, the multi-class classification procedure is split into several binary detection problems. First and foremost, a division is made into the two main modulation types, PSK and QAM. This is the first step of the classification procedure as can be seen in Figure 3.1.

In the second level, the PSK branch classifier is responsible of distinguishing between BPSK and the rest of the PSK modulations faced as a single class. Respectively, in the QAM branch the corresponding classifier distinguishes between 16-QAM and the rest of QAM modulation types in the same manner. In case the signal is classified as BPSK or 16-QAM, the classification procedure is completed. Otherwise, an additional binary classification is performed between QPSK and 8-PSK for the PSK branch or 64-QAM and 256-QAM for the QAM one.

For the sake of experimenting, different classifiers were used. Firstly, the classifier proposed in [1] was examined. During the training phase in each level, the expanded feature

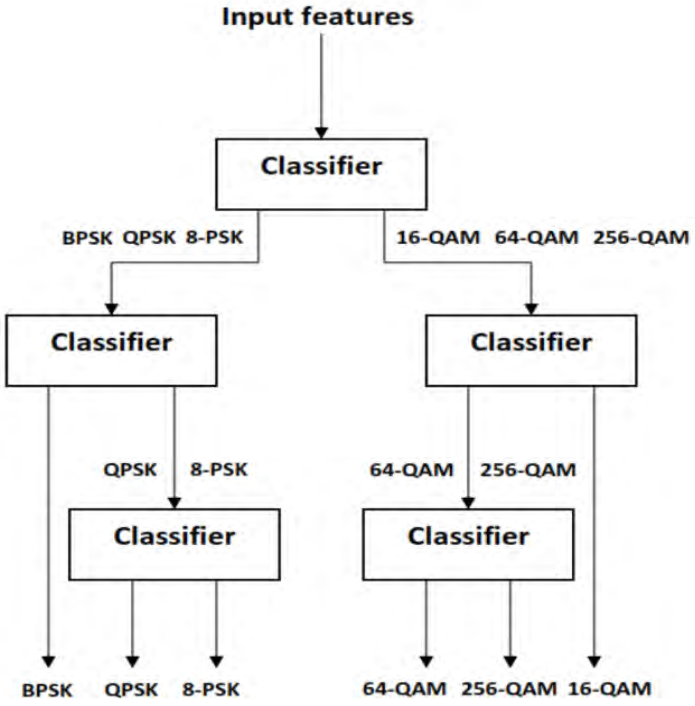

Figure 3.1: The hierarchical scheme proposed in [1]

vectors are combined, forming a matrix. Having the appropriate target values, t, the goal is to calculate the classifier weights which are selected to minimize the Mean Square Error (MSE) as:

$$w_l^c = \underset{w_l}{argmin} \|Vw_l - t_l\|^2$$

Where V is the matrix containing the expanded feature vectors and w_l^c, the corresponding level weights necessary for the classification procedure. The above equation can be rewritten in a simpler way as:

$$Vw_l^c = t_l \Rightarrow w_l^c = V^\dagger t_l$$

Note that $(\cdot)^\dagger$ stands for Moore–Penrose generalized inverse (also known as the Pseudoinverse). For example, the weights that are used for classifying a BPSK signal in the first second level of the hierarchical scheme are computed as $w_1^0 = V^\dagger t_l$. In the testing phase, the expanded feature vectors are multiplied by each node weights. The class is chosen as:

$$Class\ identity\ l = \underset{l}{argmax}\{s_l\}$$

Where s_l is the product of the expanded feature vector and the corresponding weights.

Additionally, tests were performed using the k-Nearest-Neighbors (kNN) algorithm. Proposed by Thomas Corver in 1967 [33], kNN is a non-parametric method for classification and regression. As a classification algorithm, an object is classified by a majority vote of its k neighbors and it is assigned to the class that is most common amongst them. Moreover, a number of ensemble ML algorithms were used as well. Ensemble methods use multiple but finite individually trained classifiers to obtain better predictive performance [34]. Random Forest (RF) algorithm is an ensemble method suitable for tasks such as classifying objects. Initially proposed by Tin Kam Ho [35] and later extended by Leo Breiman [36], it consists of multiple decisions trees. Using bagging and feature randomness when constructing each tree, the algorithm aims to create an uncorrelated forest of trees whose prediction by committee is more accurate than that of any individual tree. Extra-Trees (ET), proposed in [37], is another ensemble ML algorithm that was used. Similarly to the RF algorithm, it also combines the predictions from numerous decision trees, with the difference between them found in the sampling approach and the selection of cut points in order to split nodes. The third ensemble method used in our experiments was them Adaptive-Boosting, or AdaBoost. AdaBoost can be used in concurrence with other classification algorithms, also mentioned as *weak* learners. These weak models are added sequentially and trained using the weighted training data until a given number of learners are created. In the testing phase, predictions are made by calculating the weighted average of the weak models. Thus, the used classifiers can be categorized into ensemble and non-ensemble ones as seen in Table 3.1.

Non-Ensemble	Polynomial k-Nearest-Neighbors
Ensemble	Random Forests Extra Trees Adaptive-Boosting

Table 3.1: List of classifiers used in the experiments.

3.2 Simulations & Results

As mentioned in 2.3.3 two types of datasets were used. Notice that even though the number of Tx antennas is present each one of them, for the modulation classification problem, the

class is set as the *Modulation* column. The *Tx Antennas* column is disregarded in this case. Regarding the classification methods, kNN was used with the number of neighbors set equal to one. The RF and ET models were build having each 100 estimators, while the AdaBoost ones used Decision Trees (having max depth of one) as their base method. Each of them had a maximum number of estimators being equal to 100.

Splitting the dataset into 60 for training purposes and 40 for testing, we fitted and tested the suggested algorithms using as input either the extracted cumulants or the extended feature vectors (referred to as polynomial features). Their performance was evaluated in terms of accuracy. Indicative accuracy scores for each algorithm on Dataset 1 can be found in Table 3.2. A corresponding accuracy report for Dataset 2 is depicted in Table 4.2. It is evident that all classifiers performed much better in Dataset 2, where the receiver is equipped with two antennas. The most obvious reason of this happening seems to be the symbol interference that the receiver suffers in Dataset 1. When the receiver has only one antenna available, symbol interference is inevitable in the cases where the transmitter uses 2 and 4 antennas. For example in the case where 2 antennas are present in the transmitter, the incoming y symbol is written as: $y_i = h_{11}(t)x_k + h_{12}(t)x_{k+1}$. Respectively, when 4 antennas are present in the transmitter, the received y symbol is the derivative of four interfering symbols. This means that 66% of Dataset 1 contains features extracted from incoming interfered symbols which alter dramatically the statistical properties of each symbol. On the other hand, Dataset 2 possesses a much lower percentage of interfered information at 33%. Regarding each classifier's accuracy in more detail, the reader can be referred to Figures 4.2 and 4.4. The classifiers have similar performance in Dataset 1, with the worst one being the AdaBoost classifier using raw cumulant features. RF and ET algorithms presented an almost equal performance either using raw cumulants or the polynomial features. In Dataset 2, the classifiers achieve higher accuracy scores, while maintaining the same behavior. The Polynomial classifier proposed in [1] reports a lower saturation point. At the same time, RF and ET classifiers achieve scores up to 92%.

Classifier	-10dB	0dB	10dB	20dB
Polynomial	40.46	53.45	63.24	63.47
kNN (Polynomial Features)	38.5	54.97	65.74	65.74
kNN (Cumulant Features)	38.56	54.58	65.83	66.25
RF (Polynomial Features)	42.66	57.89	67.66	68.26
RF (Cumulant Features)	42.54	57.89	67.66	68.37
ET (Polynomial Features)	42.12	57.89	67.45	68.35
ET (Cumulant Features)	41.78	57.52	67.54	68.07
AdaBoost (Polynomial Features)	41.55	54.81	63.93	65.34
AdaBoost (Cumulant Features)	41.18	52.1	62.47	53.65

Table 3.2: Classification accuracy in Dataset 1.

Classifier	-10dB	0dB	10dB	20dB
Polynomial	72.93	84.74	87.8	87.83
kNN (Polynomial Features)	69.9	85.48	90.37	90.87
kNN (Cumulant Features)	69.69	85.46	90.37	90.81
RF (Polynomial Features)	74.86	87.43	91.62	92.29
RF (Cumulant Features)	74.02	87.4	91.29	91.99
ET (Polynomial Features)	74.81	87.84	91.75	92.31
ET (Cumulant Features)	74.39	87.22	91.64	92.38
AdaBoost (Polynomial Features)	73.21	85.5	89.9	91.78
AdaBoost (Cumulant Features)	73.12	84.51	90.2	90.85

Table 3.3: Classification accuracy in Dataset 2.

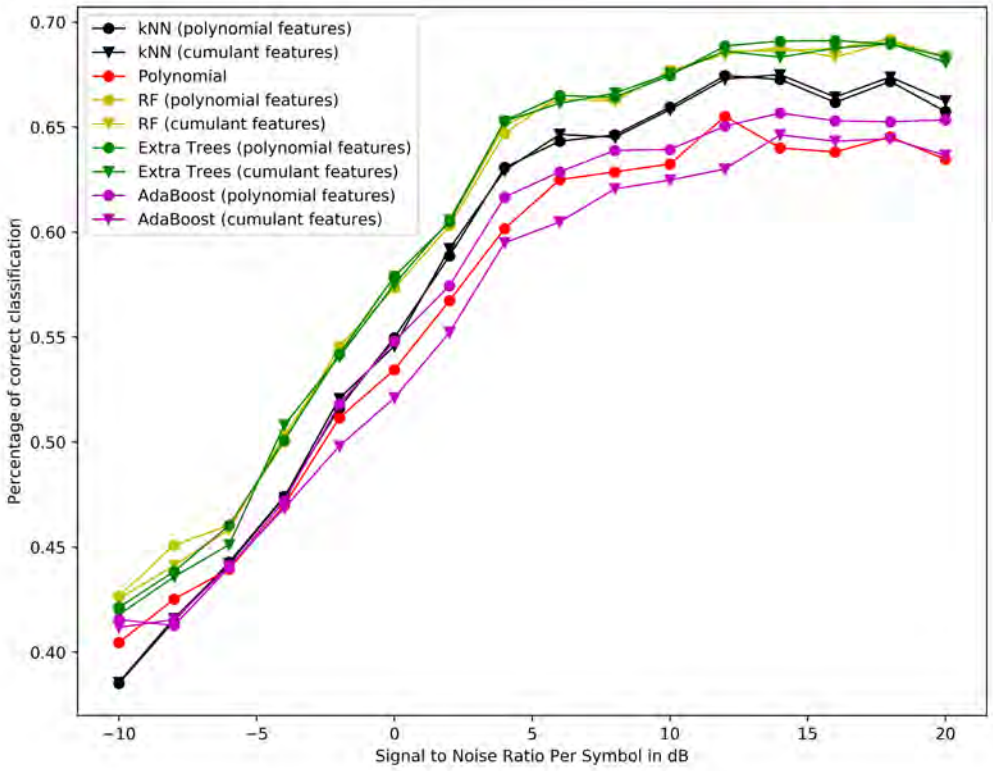

Figure 3.2: Percentage of correct classification plot on Dataset 1

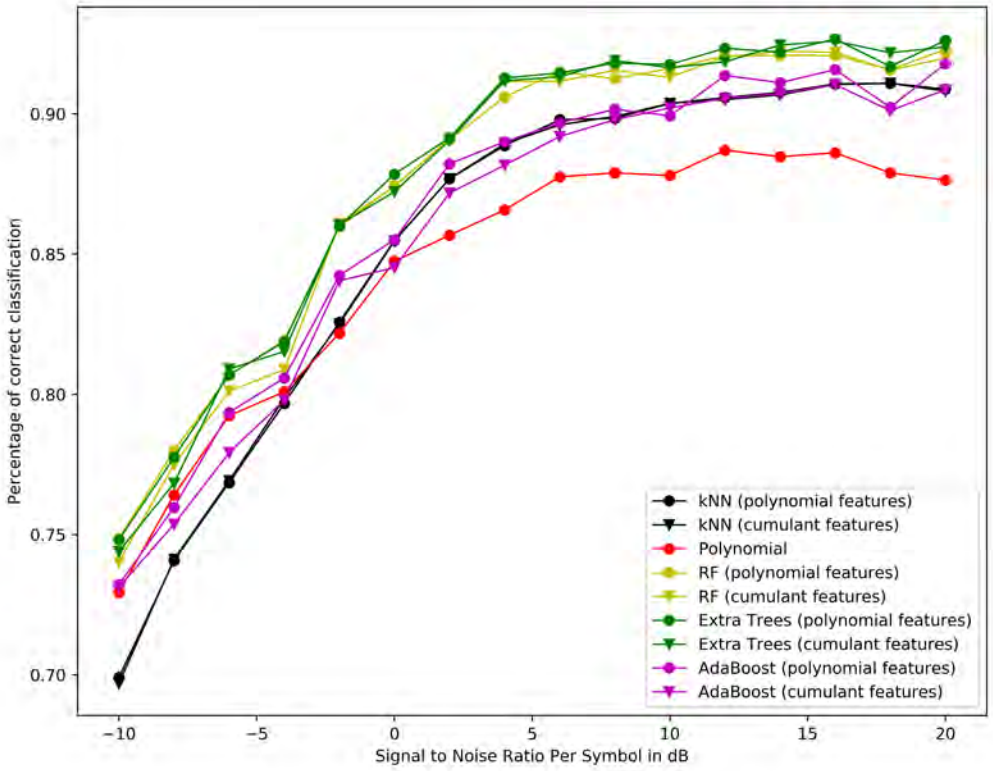

Figure 3.3: Percentage of correct classification plot on Dataset 2

Chapter 4

Number of Transmitting Antennas Classification

In this chapter, the concept of the number of Tx antennas classification is introduced. As mentioned earlier, this type of classification is a crucial part towards the transmitter configuration identification.

4.1 Problem Description

Through this scenario, the blind receiver should be able to detect the number of Tx antennas using only the raw I/Q data of the received signal. Two approaches are considered. In the first, the modulation type is totally ignored and focus is given to the classification of the number of the antennas only. On the contrary, in the second aspect the modulation type is known, and the number of Tx antennas classification is performed in a stream of data modulated in a constant way (i.e. using the BPSK modulation). Thus, one can view the classifier in the first scenario as a more *universal* one. In the second scheme, the classifiers are dedicated to each of the possible modulations present. In this way, to make the antenna detection possible throughout the second scenario, there must be knowledge on the type of modulation used. That knowledge can be passed from the transmitter to the receiver in an established communication scenario, or obtained through the modulation classification procedure described in Chapter 3.

Throughout the rest of this chapter, we will refer to the universal classifier scheme as *Scenario 1*, and to the dedicated classifier one as *Scenario 2*

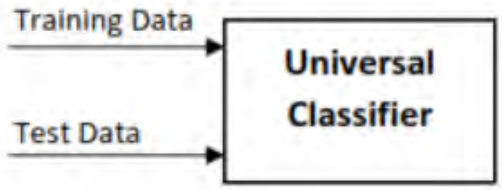

Figure 4.1: A universal classifier approach.

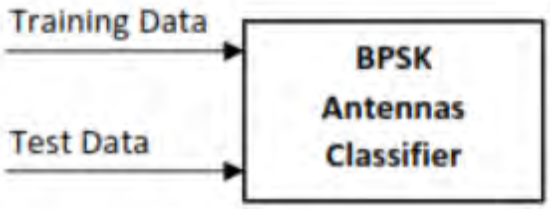

Figure 4.2: Example of a dedicated BPSK Antennas Classifier

4.2 Simulations & Results

Using the datasets mentioned in 2.3.3, the goal of this section is to examine the ability of each proposed classification scheme in detecting the number of antennas used by the transmitter. For both scenarios, kNN classifier was used, having the number of neighbors set to 5. RF was tested, having 100 estimators, while ET was equipped with 200. Finally, AdaBoost was used having RF with 100 estimators as its base method. In *Scenario 1*, the *Modulation* column is disgarded completely, as the modulation type of the received signal is not taken into consideration. On the other hand, in *Scenario 2*, the modulation type plays a major role in the construction of the necessary classifiers. Thus, the dataset is split into six groups (the same number as the number of the available modulations) and each one assists in the creation of a corresponding classification model. The performance of each classifier is evaluated in terms of their accuracy as done in the previous chapter.

4.2.1 The Universal Classifier

Using a train-test split of 60%-40%, the classification algorithms were trained on 6480 samples and tested on 4320. It is evident that the ensemble methods (RF, ET, AdaBoost) performed considerably better than the kNN classifier in both datasets especially in low SNR

values. Examining the percentage of correct classification plot in Figure 4.3, the fact that using multiple Rx antennas contributes to a higher classification accuracy score is proven. This is more evident in low SNR values, such as -10, where a rise up to 14.56% in classification accuracy is spotted. In higher SNR values, such as 20, there is still an important rise of 5.51% (in the kNN classifier). In table, the reader can have an analytical report of the accuracy scores in a variety of SNR values.

Classifier	-10dB	0dB	10dB	20dB
kNN	56.96	75.32	85.09	85.32
RF	61.82	79.37	87.12	87.52
ET	62.17	79.46	87.43	88.1
AdaBoost	62.77	78.95	87.08	87.66

Table 4.1: Classification accuracy in Dataset 1 - Scenario 1.

Classifier	-10dB	0dB	10dB	20dB
kNN	71.52	85.53	90.76	90.83
RF	76.31	87.8	91.41	91.75
ET	76.41	88.72	92.59	92.84
AdaBoost	75.94	88.05	91.43	92.26

Table 4.2: Classification accuracy in Dataset 2 - Scenario 1.

4.2.2 Dedicated Tx Antennas Classifiers

Even though the *Universal* classifier proposed in the previous subsection performed considerably well, multiple classifiers dedicated to each of the available modulation scheme were tested. This leads to the creation of a total of six classifiers for every SNR value. Using the same split between train and test set as in 4.2.1, less data is used in the training process, since each classifier is trained on 1080 samples and tested on 720. The classifiers were evaluated in both Dataset 1 and Dataset 2 and analytical accuracy reports can be found in Tables 4.3 to 4.6. The usage of two antennas by the receiver benefits the QAM modulations to a great extent (Table 4.6) especially in lower SNR values where a rise of up to 45.14% is spotted at

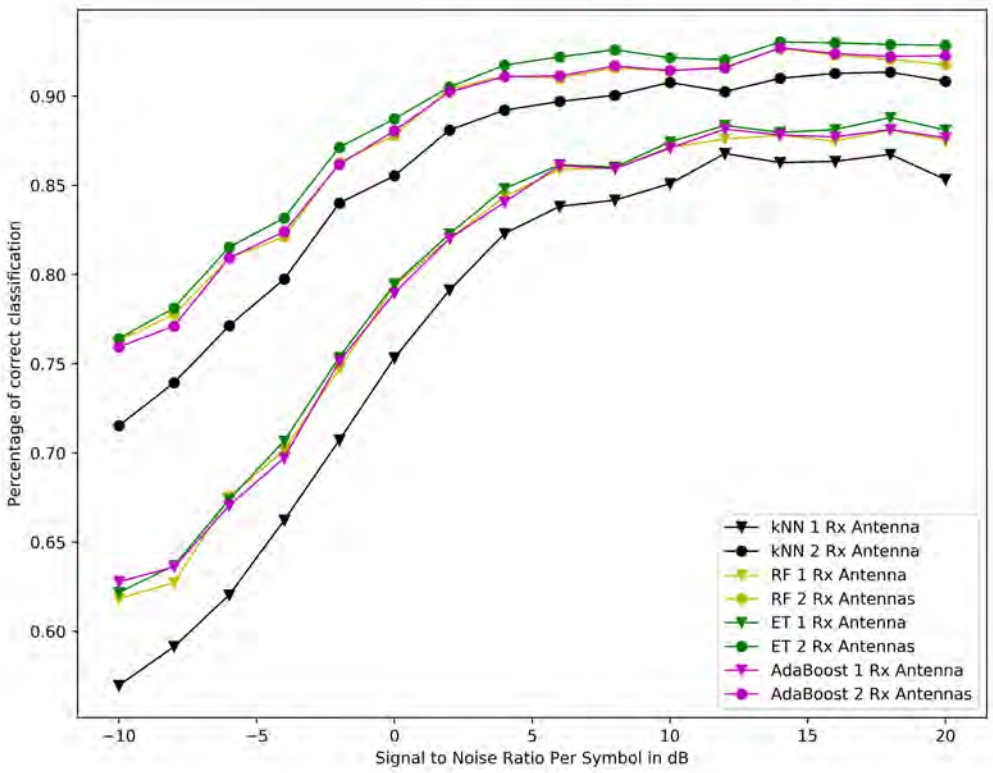

Figure 4.3: Percentage of Correct Classification in both datasets - Scenario 1.

-10dB. What can be spotted right away, is that the 16QAM modulation achieves a very high accuracy score, even with the presence of only one antenna in the receiver as seen in 4.5. Pair-plotting the corresponding features in a concept where the SNR value is equal to -10dB (Figure 4.7), proved that the features are in fact more distinguishable (as are their distributions over the available classes) than the ones derived from a BPSK modulated signal (Figure 4.6). Comparing these two pair plots, it is easy to conclude that, through their distributions, the 16QAM features are more likely to be classified correctly.

Modulation	Classifier	-10dB	0dB	10dB	20dB
BPSK	KNN	55.5	90.5	97.08	97.08
	RF	60.55	93.47	97.63	97.22
	ET	60.55	93.19	97.63	98.05
	AdaBoost	60.55	92.91	97.36	97.5
QPSK	KNN	61.94	95	97.91	97.22
	RF	64.44	95.69	97.91	97.36
	ET	63.33	95.83	98.19	97.63
	AdaBoost	63.19	95.83	97.5	97.91
8-PSK	KNN	72.08	93.75	95.83	95.13
	RF	78.47	94.44	95.69	96.11
	ET	78.05	94.72	96.25	95.83
	AdaBoost	77.63	94.44	96.66	96.25

Table 4.3: Classification accuracy in Dataset 1 for PSK dedicated classifiers.

Modulation	Classifier	-10dB	0dB	10dB	20dB
16-QAM	KNN	86.52	94.72	96.52	96.94
	RF	91.66	94.86	96.94	97.91
	ET	91.38	95.69	97.36	97.77
	AdaBoost	91.11	95.13	97.08	97.91
64-QAM	KNN	61.94	95	97.91	97.22
	RF	64.44	95.69	97.91	97.36
	ET	63.33	95.83	98.19	97.63
	AdaBoost	63.19	95.83	97.5	97.91
256-QAM	KNN	51.8	90.13	96.25	96.52
	RF	56.52	90.97	95.97	97.22
	ET	57.63	92.22	95.55	96.94
	AdaBoost	57.63	91.52	95.83	97.08

Table 4.4: Classification accuracy in Dataset 1 for QAM dedicated classifiers.

Modulation	Classifier	-10dB	0dB	10dB	20dB
BPSK	KNN	52.77	94.16	98.47	99.3
	RF	60.41	94.58	98.88	99.58
	ET	60.69	95	98.88	99.58
	AdaBoost	60.55	96.66	98.75	99.58
QPSK	KNN	65.55	97.83	99.58	99.3
	RF	72.63	97.91	99.16	99.3
	ET	71.25	98.05	99.58	99.44
	AdaBoost	71.25	97.77	99.3	99.16
8-PSK	KNN	73.33	97.63	98.47	98.33
	RF	79.72	97.63	98.75	98.88
	ET	81.66	98.19	98.61	99.44
	AdaBoost	80.55	97.77	98.61	98.88

Table 4.5: Classification accuracy in Dataset 2 for PSK dedicated classifiers.

Modulation	Classifier	-10dB	0dB	10dB	20dB
16-QAM	KNN	92.22	97.77	98.61	98.33
	RF	94.44	98.19	98.75	98.75
	ET	94.44	98.61	98.88	98.61
	AdaBoost	94.3	98.33	98.61	98.61
64-QAM	KNN	96.52	96.8	98.19	96.94
	RF	98.05	98.05	98.88	98.05
	ET	98.33	98.33	98.75	98.19
	AdaBoost	97.77	97.91	98.8	98.05
256-QAM	KNN	96.94	96.38	97.91	97.91
	RF	98.47	98.19	99.16	98.61
	ET	98.33	98.47	99.44	98.88
	AdaBoost	98.33	98.05	99.16	98.61

Table 4.6: Classification accuracy in Dataset 2 for QAM dedicated classifiers.

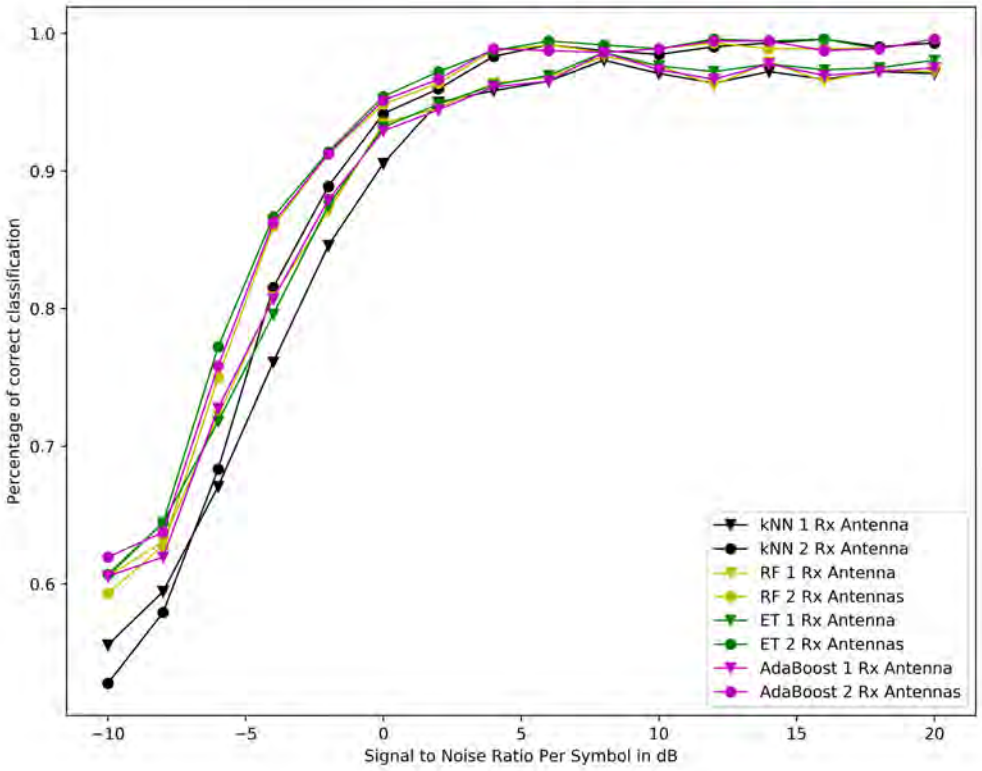

Figure 4.4: No. of Antennas Classification in BPSKs modulated signals

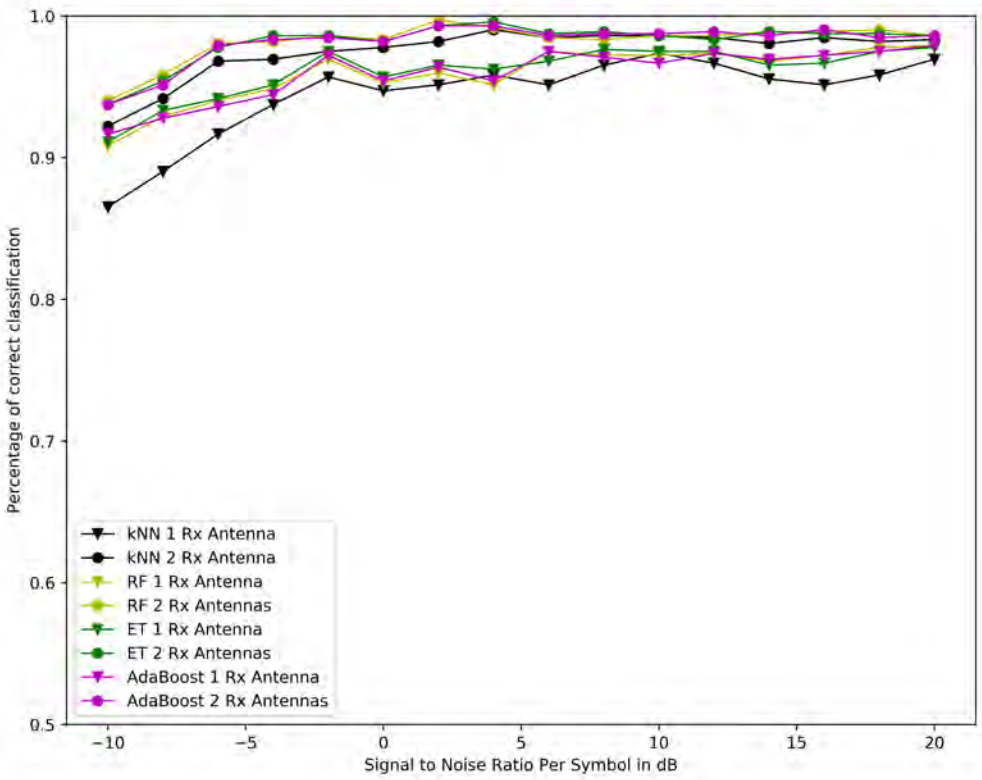

Figure 4.5: No. of Antennas Classification in 16QAM modulated signals

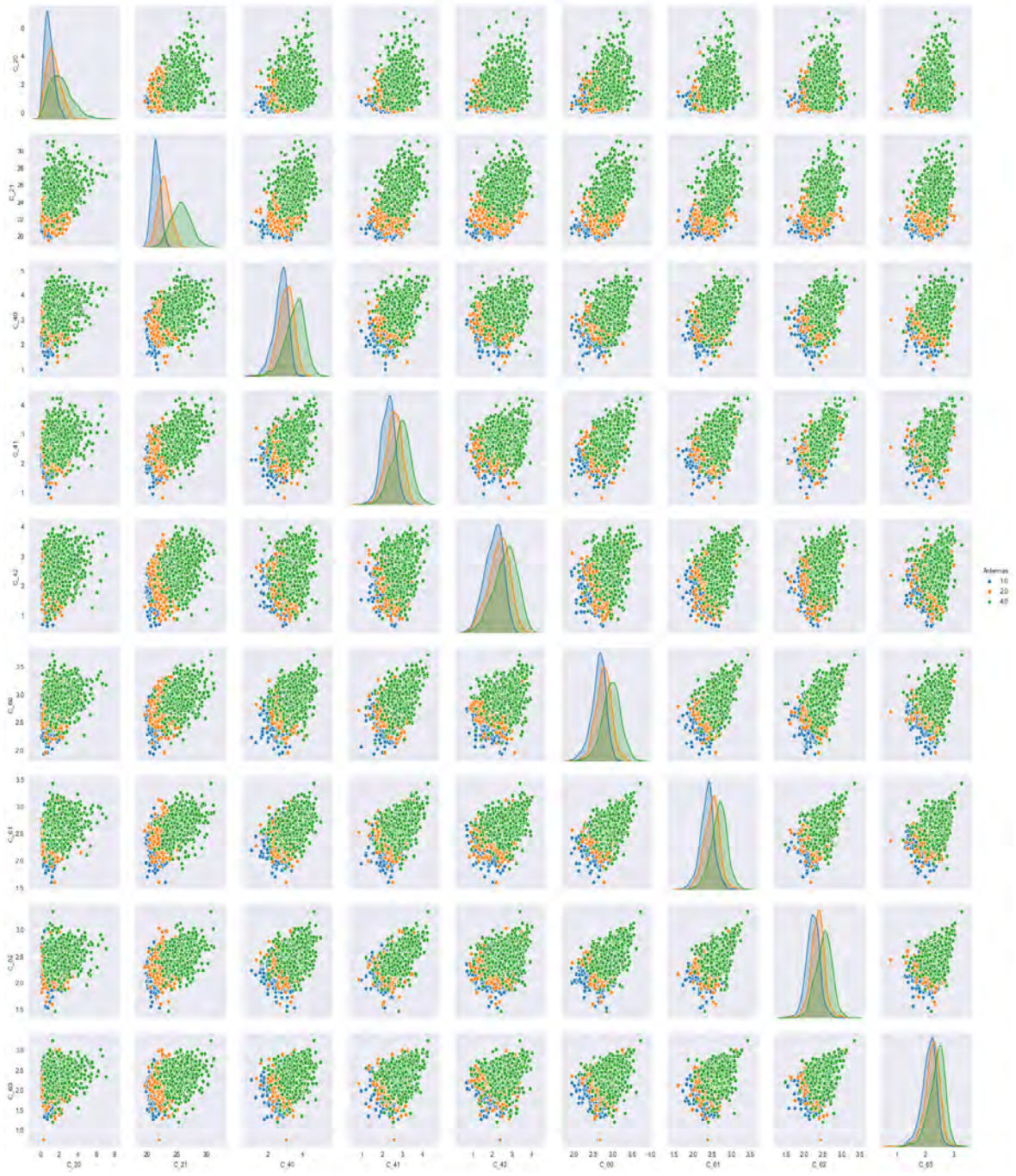

Figure 4.6: Pair plot of features found in BPSK modulated signals

Figure 4.7: Pair plot of features found in 16QAM modulated signals

Chapter 5

Joint Classification

In this chapter, the joint nature of signal classification is examined. In Chapters 3 and 4, the problems of modulation and antennas classification, respectively, were addressed separately as independent procedures. Combining the two procedures, one joint classifier can emerge. In the following two sections, the two different approaches discussed in Chapter 4 are applied to form each joint classifier.

5.1 Joint Classification Using the Universal Classifier

In this type of joint classification, the two parts composing it can be viewed as independent. That is since the antennas detection procedure is not subject to the modulation classification results. Thus, as seen in Figure 5.1, during the training stage, both classifiers are provided with the same training data. What differs their training processes, are the corresponding target values. In the case of the Hierarchical Modulation Classifier, the target values in the training procedure are present in the *Modulation* column of each dataset used. During this procedure, the *Antennas* column is ignored. Simultaneously, the training of the antennas classifier is taking place, this time using the values of the *Antennas* column as target values.

The independence between these two classifiers is mainly found during the testing phase. Once again, provided the same test set, predictions are made by each model separately. The Hierarchical Modulation model will predict the modulation type of each received signal. In the same time, the Universal Antenna Classifier model makes predictions on the number of Tx antennas for each signal contained in the test set. Then, the predictions are combined in a two column matrix and compared with the true corresponding values. In this work, we used

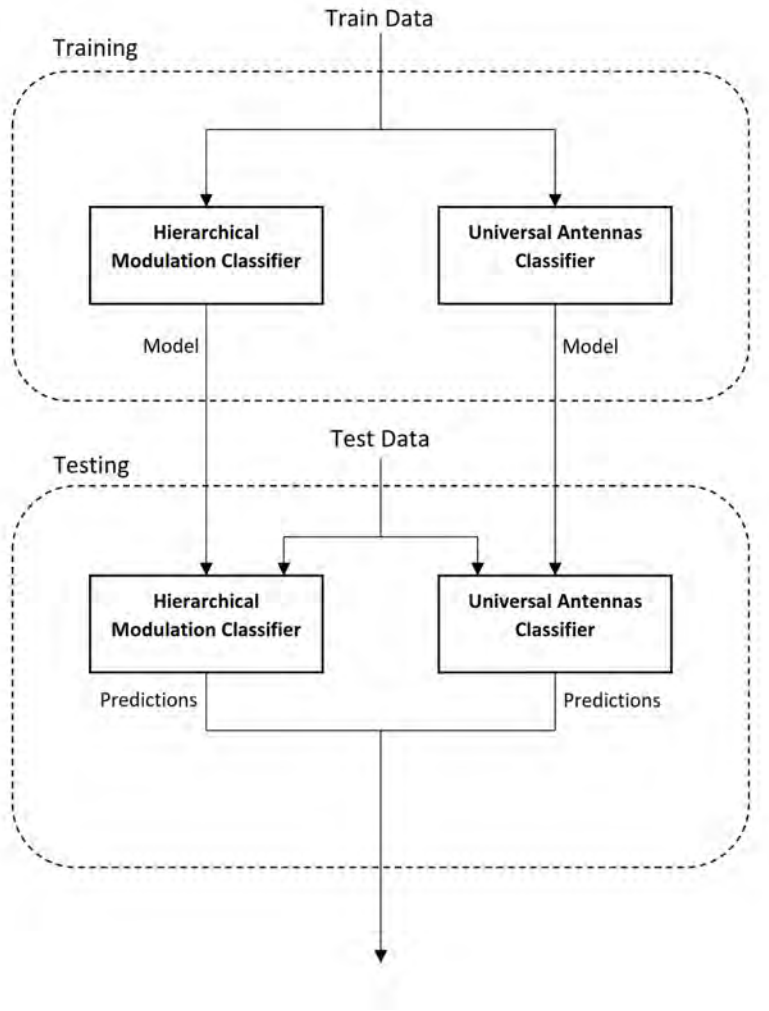

Figure 5.1: The proposed joint classifier using the Universal concept in No. of antennas classification

the same type of classification algorithm for both the modulation and antennas classifier.

5.2 Joint Classification Using Dedicated Classifiers

As discussed in Chapter 4, the antennas classification problem can be dealt with creating classifiers dedicated to each modulation type present. Unlike the *Universal* approach of the previous section, where one model is built classifying the number of antennas regardless of the way the signal is modulated, in this approach six different models are being created. Once again, the training stage can be seen as an independent procedure for the two different classifier types. As in Section 5.1, the Hierarchical Modulation Classifier is trained, having the *Modulation* column as its target values. On the other hand, the training of each dedicated classifier requires the fitting of six different models. Hence, the train data is split into six

parts according to the corresponding modulation type. In this way, the dedicated antennas classifiers are constructed.

During the testing procedure, a pipeline shown in Figure 5.2 is followed. It should be noted that for the dedicated models to work properly, data with constant modulation type should be used as input. First the modulation classification takes place, and with the predictions made by the corresponding model the test set is split into six parts depending on the classified modulation type. It is then up to each antennas classification model to effectively classify the No. of antennas transmitting the received signal. Finally, the No. of antennas predictions are combined with the modulation classification ones to form a two column matrix that will make the derivation of the joint classification accuracy possible.

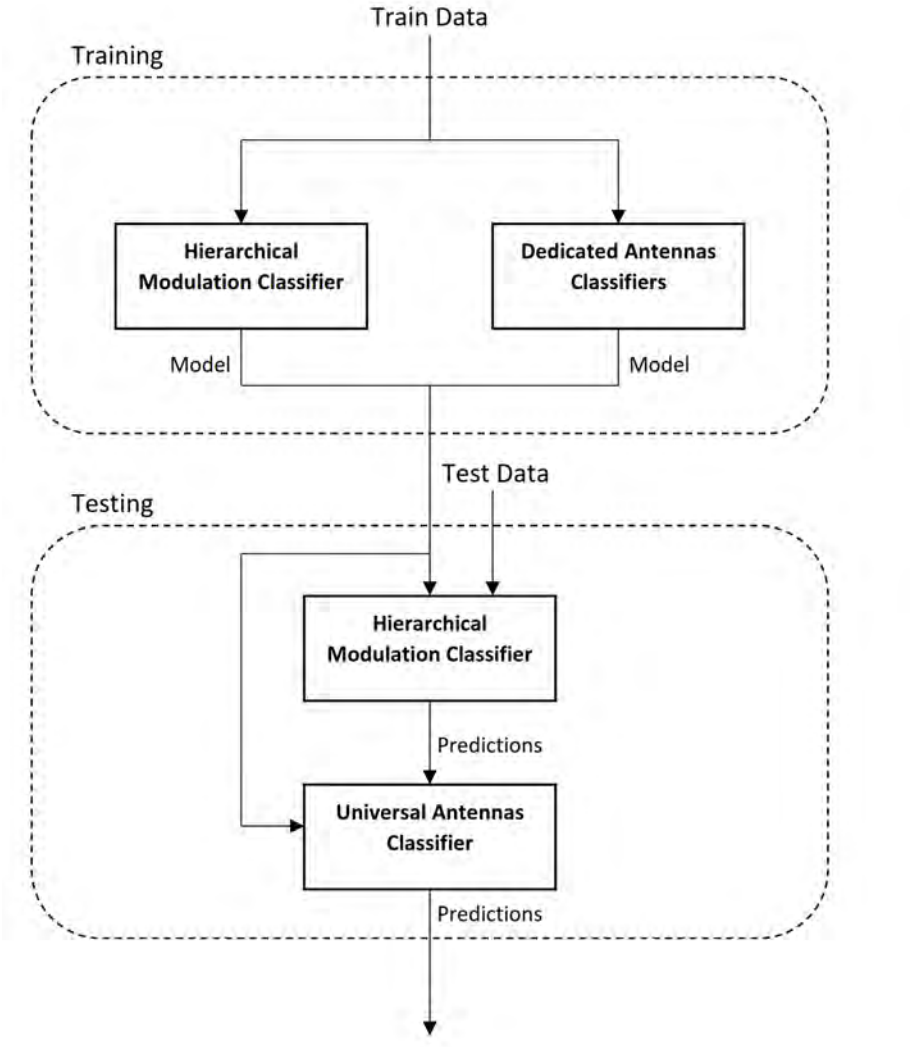

Figure 5.2: The proposed joint classifier using the Dedicated Classifiers concept in No. of antennas classification

5.3 Simulations & Results

As done in the previous chapters, *Dataset 1* and *Dataset 2* are used in order to provide insight into whether a diversity in the number of Tx antennas leads to better classification accuracy. The train-test split is set to 60%-40% as in every experiment run in the course of this thesis. The classification algorithms are cosen to be kNN with 100 neighbours, RF with 100 estimators, ET with 200 estimators and AdaBoost classifier having 100 estimators and the previously described RF model as its base estimator. These models are used both in the Hierarchical Modulation and the Antennas classifiers, universal or not.

For simplicity reasons, we refer to the proposed signal classifier with the *Universal* antennas classifier as *Classifier 1*, and to the one with the multiple *Dedicated* antennas classifier as *Classifier 2*.

Starting with the scenario involving *Classifier 1*, the contribution of multiple antennas usage is evident as can be seen in Figure 5.3. From the results presented in the previous chapters, it was expected that the use of two antennas at the receiver would result in a rise of the classification accuracy in the joint scenario as well. For once more, the use of two Rx antennas improved the performance by a percentage up to 26%, with the most notable improvement spotted in low SNR values. For example, kNN algorithm achieves an accuracy score of 26.22% in -10dB using one antenna, while the accuracy reaches up to 58.5% in the same SNR conditions using two Rx antennas. Experiments do not show any particular advantage in using a certain classification algorithm over the others, since their performances are almost identical. The only exception is kNN, which seems to underperform slightly in lower SNR values. The reader may refer to Tables 5.3 and 5.4 for a more detailed report on the classification accuracy in *Dataset 1* and *Dataset 2* respectively.

Classifier	-10dB	0dB	10dB	20dB
kNN	26.22	48.91	63.12	63.14
RF	30.32	50.94	64.05	64.35
ET	30.23	51.34	64.81	65.16
AdaBoost	29.32	51.27	63.57	64.42

Table 5.1: Classification accuracy in Dataset 1 regarding Classifier 1.

In the second scenario, where dedicated classifiers for each modulation are present, the

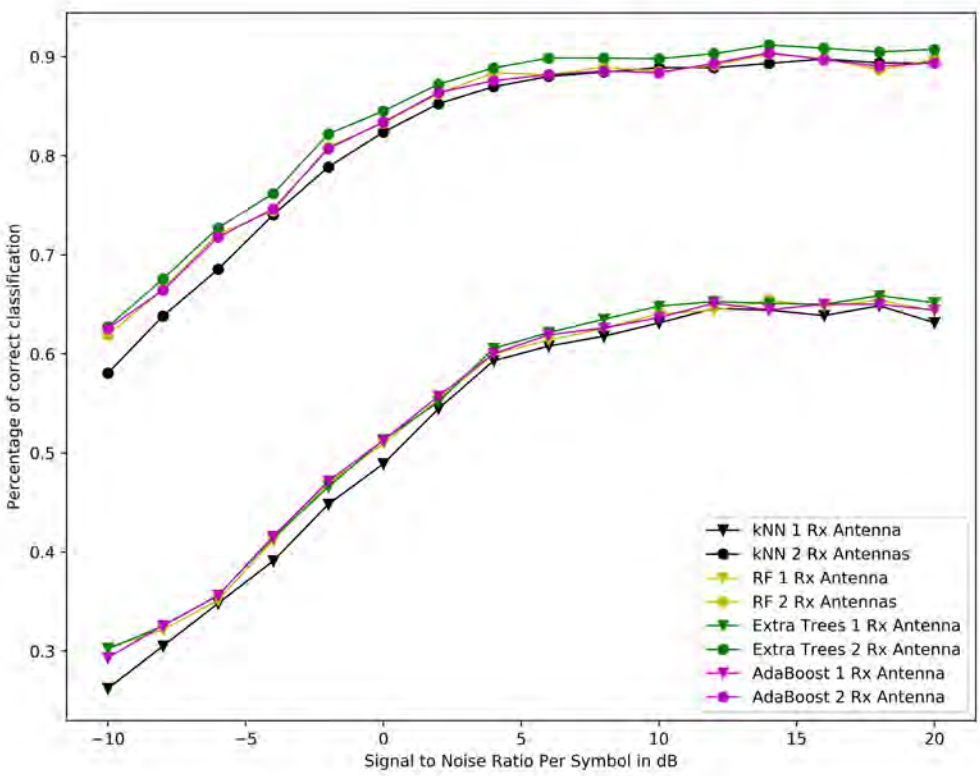

Figure 5.3: Percentage of correct classification for Classifier 1

Classifier	-10dB	0dB	10dB	20dB
kNN	58.05	82.38	88.88	89.37
RF	61.89	83.31	88.49	89.72
ET	62.73	84.51	89.79	90.74
AdaBoost	62.56	83.4	88.37	89.37

Table 5.2: Classification accuracy in Dataset 2 regarding Classifier 1.

same behavior can be spotted regarding the multiple antennas contribution. For once more, it is proven in Figure 5.4 that diversity the number of Rx antennas leads to better classification accuracy. What is more clear in this scenario, is the underperformance of the kNN algorithm, at least in lower SNR values.

What would be interesting to examine is the improvement that the use of the dedicated classifiers induces to the overall classification performance. In Figures 5.5 and 5.6 it is proved

that indeed by using dedicated classifiers, a higher classification accuracy can be achieved even in its slightest form.

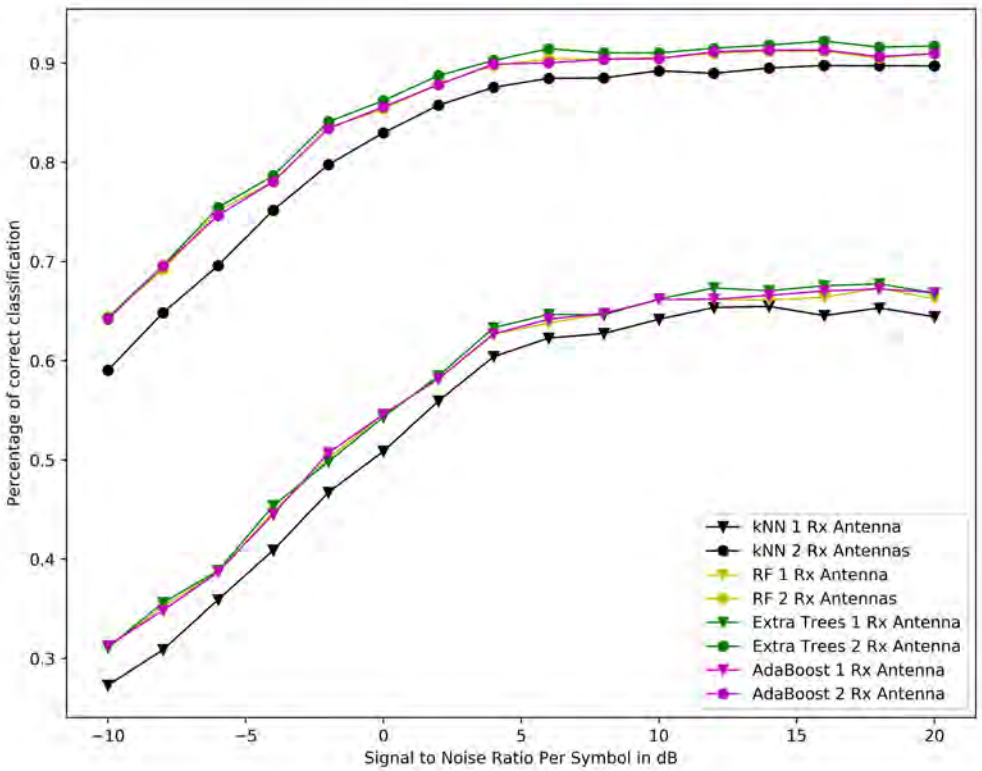

Figure 5.4: Percentage of correct classification for Classifier 2

Classifier	-10dB	0dB	10dB	20dB
kNN	27.29	50.87	64.18	64.44
RF	31.08	54.6	66.18	66.22
ET	31.08	54.32	66.22	66.82
AdaBoost	31.27	54.6	66.18	66.87

Table 5.3: Classification accuracy in Dataset 1 regarding Classifier 2.

Classifier	-10dB	0dB	10dB	20dB
kNN	59.05	82.98	89.23	89.72
RF	64.42	85.39	90.55	91.01
ET	64.32	86.22	91.04	91.73
AdaBoost	64.21	85.6	90.46	90.94

Table 5.4: Classification accuracy in Dataset 2 regarding Classifier 2.

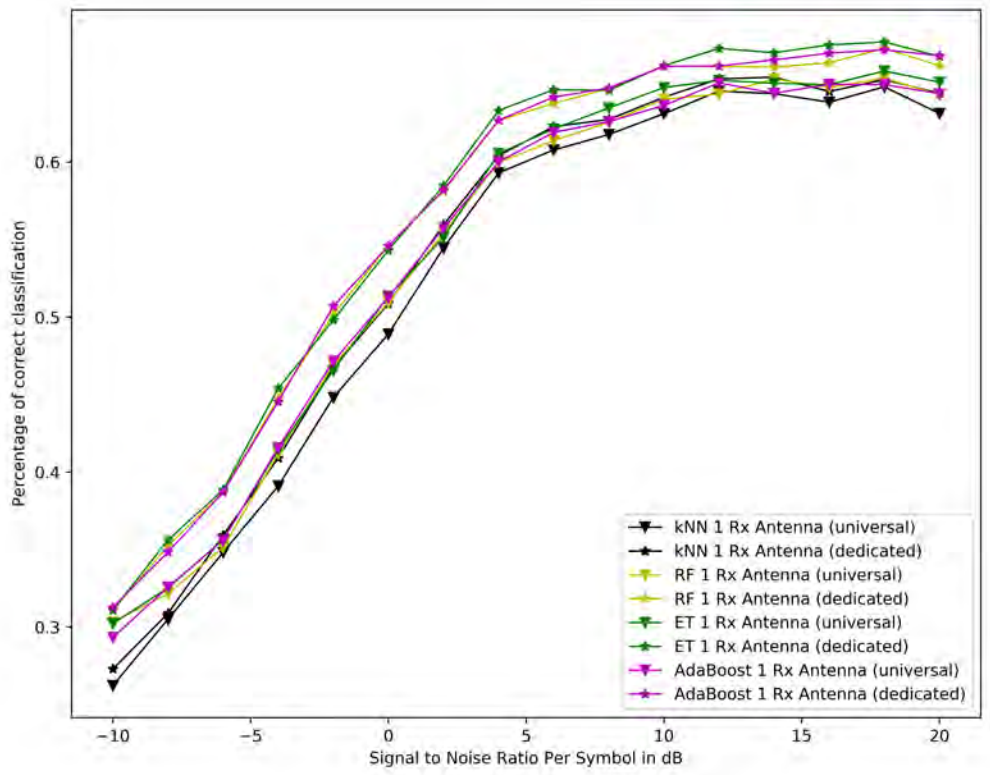

Figure 5.5: Comparison of the two Classifiers in Dataset 1

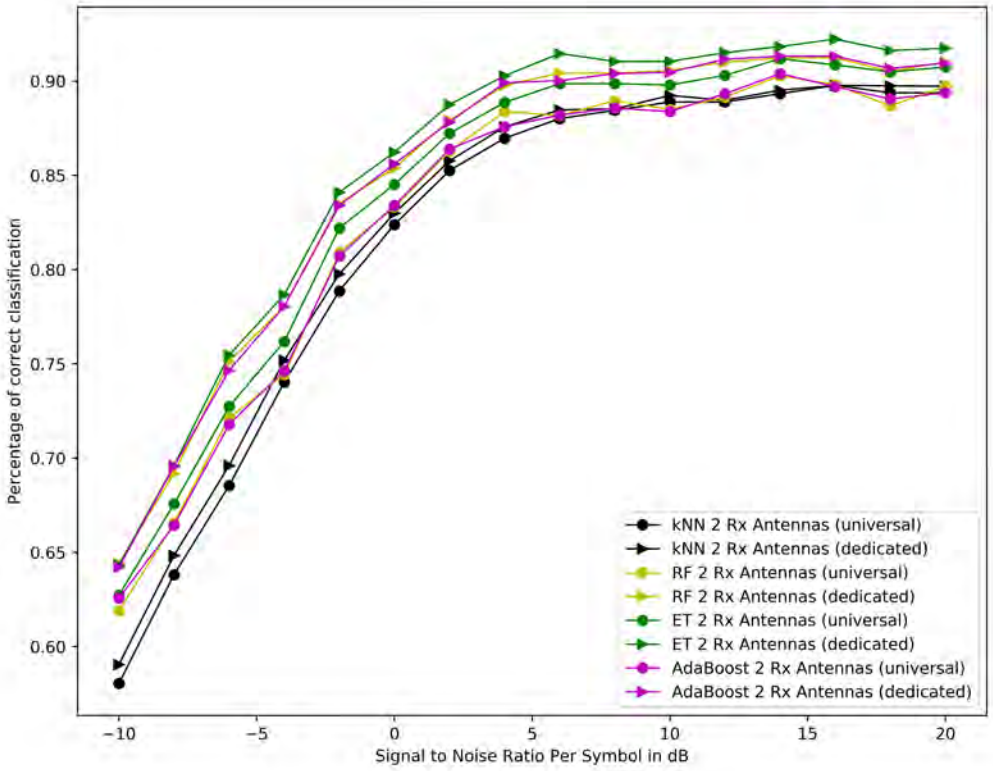

Figure 5.6: Comparison of the two Classifiers in Dataset 2

Chapter 6

Conclusion & Future Work

In the span of this work, the signal classification problem was tackled. Considering its nature, signal classification was treated as a multidimensional concept, splitting it into two categories: Modulation and Antennas Classification. To acquire the much needed data for our experimentation, a simulator was developed using MATLAB programming language. The simulator simulates the transmission of a signal from the transmitter through the fading channel. Through it, the I/Q data is received, leading to the feature extraction which consists of the HOCs calculation. Having the dataset containing the corresponding features for each transmitted signal, the classification problems were initially examined separately. It was proved that the classification performance was strongly correlated with the SNR values in both cases. It was also proved that a diversity in the number of Rx antennas results to a considerably better classification accuracy. During the joint classification experiments, it was shown that classifiers using dedicated antennas classification models for each modulation type performed slightly better than the ones using the universal antennas classifier. The concept of signal classification and its derivatives could be examined further using more state-of-the-art algorithms. As a future step, concepts such as transmitter localization, or equipment identification could be examined. Furthermore, another scenario worth analyzing is the one where the transmitter is trying to affect the classification performance via spoofing attacks.

Bibliography

[1] Ameen Abdelmutalab, Khaled Assaleh, and Mohamed El-Tarhuni. Automatic modulation classification based on high order cumulants and hierarchical polynomial classifiers. *Physical Communication*, 21:10–18, 2016.

[2] Zhechen Zhu and Asoke K Nandi. *Automatic modulation classification: principles, algorithms and applications*. John Wiley & Sons, 2015.

[3] Ananthram Swami and Brian M Sadler. Hierarchical digital modulation classification using cumulants. *IEEE Transactions on communications*, 48(3):416–429, 2000.

[4] Sreeraj Rajendran, Wannes Meert, Domenico Giustiniano, Vincent Lenders, and Sofie Pollin. Deep learning models for wireless signal classification with distributed low-cost spectrum sensors. *IEEE Transactions on Cognitive Communications and Networking*, 4(3):433–445, 2018.

[5] Víctor Iglesias, Jesós Grajal, and Omar Yeste-Ojeda. Automatic modulation classifier for military applications. In *2011 19th European Signal Processing Conference*, pages 1814–1818. IEEE, 2011.

[6] Octavia A Dobre, Ali Abdi, Yeheskel Bar-Ness, and Wei Su. Survey of automatic modulation classification techniques: classical approaches and new trends. *IET communications*, 1(2):137–156, 2007.

[7] Timothy O'Shea and Jakob Hoydis. An introduction to deep learning for the physical layer. *IEEE Transactions on Cognitive Communications and Networking*, 3(4):563–575, 2017.

[8] Fan Meng, Peng Chen, Lenan Wu, and Xianbin Wang. Automatic modulation classification: A deep learning enabled approach. *IEEE Transactions on Vehicular Technology*, 67(11):10760–10772, 2018.

[9] Yu Wang, Jie Yang, Miao Liu, and Guan Gui. Lightamc: Lightweight automatic modulation classification via deep learning and compressive sensing. *IEEE Transactions on Vehicular Technology*, 69(3):3491–3495, 2020.

[10] Duona Zhang, Wenrui Ding, Baochang Zhang, Chunyu Xie, Hongguang Li, Chunhui Liu, and Jungong Han. Automatic modulation classification based on deep learning for unmanned aerial vehicles. *Sensors*, 18(3):924, 2018.

[11] Sharan Ramjee, Shengtai Ju, Diyu Yang, Xiaoyu Liu, Aly El Gamal, and Yonina C Eldar. Fast deep learning for automatic modulation classification. *arXiv preprint arXiv:1901.05850*, 2019.

[12] Afan Ali and Fan Yangyu. Unsupervised feature learning and automatic modulation classification using deep learning model. *Physical Communication*, 25:75–84, 2017.

[13] Timothy J O'Shea, Johnathan Corgan, and T Charles Clancy. Convolutional radio modulation recognition networks. In *International conference on engineering applications of neural networks*, pages 213–226. Springer, 2016.

[14] Hoda Ayatollahi, Cristiano Tapparello, and Wendi Heinzelman. Transmitter-receiver energy efficiency: A trade-off in mimo wireless sensor networks. In *2015 IEEE wireless communications and networking conference (WCNC)*, pages 1476–1481. IEEE, 2015.

[15] Eckhard Ohlmer, Ting-Jung Liang, and Gerhard Fettweis. Algorithm for detecting the number of transmit antennas in mimo-ofdm systems: receiver integration. In *2008 IEEE 68th Vehicular Technology Conference*, pages 1–5. IEEE, 2008.

[16] Jon Hamkins. Autonomous receiver configuration.

[17] Mohamed-Rabie Oularbi, Saeed Gazor, Abdeldjalil Aissa-El-Bey, and Sebastien Houcke. Enumeration of base station antennas in a cognitive receiver by exploiting pilot patterns. *IEEE communications letters*, 17(1):8–11, 2012.

[18] Mohamed-Rabie Oularbi, Saeed Gazor, Abdeldjalil Aissa-El-Bey, and Sébastien Houcke. Exploiting the pilot pattern orthogonality of ofdma signals for the estimation of base stations number of antennas. In *2013 8th International Workshop on Systems, Signal Processing and their Applications (WoSSPA)*, pages 465–470. IEEE, 2013.

[19] Oren Somekh, Osvaldo Simeone, Yeheskel Bar-Ness, and Wei Su. Detecting the number of transmit antennas with unauthorized or cognitive receivers in mimo systems. In *MILCOM 2007-IEEE Military Communications Conference*, pages 1–5. IEEE, 2007.

[20] Merve Turan, Mengüç Öner, and Hakan Ali Çırpan. Joint modulation classification and antenna number detection for mimo systems. *IEEE Communications Letters*, 20(1):193–196, 2015.

[21] David Tse and Pramod Viswanath. *Fundamentals of wireless communication*. Cambridge university press, 2005.

[22] Fahed Hameed, Octavia A Dobre, and Dimitrie C Popescu. On the likelihood-based approach to modulation classification. *IEEE Transactions on Wireless Communications*, 8(12):5884–5892, 2009.

[23] K Assaleh, K Farrell, and RJ Mammone. A new method of modulation classification for digitally modulated signals. In *MILCOM 92 Conference Record*, pages 712–716. IEEE, 1992.

[24] Wu Dan, Gu Xuemai, and Guo Qing. A new scheme of automatic modulation classification using wavelet and wsvm. 2005.

[25] Fangjuan Xie, Chisheng Li, and Guojin Wan. An efficient and simple method of mpsk modulation classification. In *2008 4th International Conference on Wireless Communications, Networking and Mobile Computing*, pages 1–3. IEEE, 2008.

[26] Shengliang Peng, Hanyu Jiang, Huaxia Wang, Hathal Alwageed, Yu Zhou, Marjan Mazrouei Sebdani, and Yu-Dong Yao. Modulation classification based on signal constellation diagrams and deep learning. *IEEE transactions on neural networks and learning systems*, 30(3):718–727, 2018.

[27] Negar Ahmadi. Using fuzzy clustering and ttsas algorithm for modulation classification based on constellation diagram. *Engineering Applications of Artificial Intelligence*, 23(3):357–370, 2010.

[28] Xin Zhou, Ying Wu, and Bin Yang. Signal classification method based on support vector machine and high-order cumulants. *Wirel. Sens. Netw.*, 2(1):48–52, 2010.

[29] Luokun Liu and Jiadong Xu. A novel modulation classification method based on high order cumulants. In *2006 International Conference on Wireless Communications, Networking and Mobile Computing*, pages 1–5. IEEE, 2006.

[30] Wei Su. Feature space analysis of modulation classification using very high-order statistics. *IEEE Communications Letters*, 17(9):1688–1691, 2013.

[31] Octavia A Dobre, Yeheskel Bar-Ness, and Wei Su. Higher-order cyclic cumulants for high order modulation classification. In *IEEE Military Communications Conference, 2003. MILCOM 2003.*, volume 1, pages 112–117. IEEE, 2003.

[32] Nathan P Geisinger. Classification of digital modulation schemes using linear and nonlinear classifiers. Technical report, NAVAL POSTGRADUATE SCHOOL MONTEREY CA, 2010.

[33] Thomas Cover and Peter Hart. Nearest neighbor pattern classification. *IEEE transactions on information theory*, 13(1):21–27, 1967.

[34] David Opitz and Richard Maclin. Popular ensemble methods: An empirical study. *Journal of artificial intelligence research*, 11:169–198, 1999.

[35] Tin Kam Ho. Random decision forests. In *Proceedings of 3rd international conference on document analysis and recognition*, volume 1, pages 278–282. IEEE, 1995.

[36] Leo Breiman. Random forests. *Machine learning*, 45(1):5–32, 2001.

[37] Pierre Geurts, Damien Ernst, and Louis Wehenkel. Extremely randomized trees. *Machine learning*, 63(1):3–42, 2006.